

Date of publication xxxx 00, 0000, date of current version xxxx 00, 0000.

Digital Object Identifier 10.1109/ACCESS.2017.DOI

Comprehensive study and comparison on 5G NOMA schemes

ZHANJI WU¹, KUN LU¹, CHENGXIN JIANG¹, AND XUANBO SHAO¹

¹School of Information and Communication Engineering, Beijing University of Posts and Telecommunications, Beijing 100876, China

Corresponding author: Zhanji Wu (e-mail: wuzhanji@bupt.edu.cn).

This work is sponsored by the National Natural Science Fund (61171101) and the Fundamental Research Funds for the Central Universities of China.

ABSTRACT Compared to the traditional orthogonal multiple access (OMA), non-orthogonal multiple access (NOMA) technology can achieve higher spectrum efficiency and support more massive connectivity. In this article, we conduct comprehensive study and comparison on current NOMA technologies that many mainstream companies have proposed for the fifth generation (5G) wireless communication standard. According to the characteristics of the NOMA schemes, we classify these schemes into four categories: scrambling-based NOMA, spreading-based NOMA, coding-based NOMA and interleaving-based NOMA. We systematically summarize the transceiver block diagram of each category, and detail basic principles, key features and transmission-reception algorithms of all NOMA schemes. Furthermore, the theoretical analysis based on average mutual information is given to evaluate the achievable sum-rate performance of the NOMA systems and their potential performance gains as compared with OMA. Comprehensive simulations are carried out for the block-error-rate (BLER) performance evaluation of these NOMA schemes as well, which coincide with the theoretical analysis. By comparing the performance of these technologies, some promising schemes and directions are suggested for the future 5G NOMA development.

INDEX TERMS NOMA, 5G, scrambling, spreading, coding, interleaving.

I. INTRODUCTION

WITH the rapid development of mobile Internet of things (IoT), much more user equipments (UEs) and much higher data-rate pose big challenges for the future mobile wireless network. In 2014, the international mobile telecommunication (IMT)-2020 promotion group proposed the vision and requirements of the fifth generation (5G) wireless communication. The 5G system aims to support much higher spectral efficiency (SE) and much more massive connectivity, and new non-orthogonal multiple access (NOMA) is one key technology to meet these strict requirements [1]–[4]. The typical application scenarios of 5G consist of enhanced Mobile BroadBand (eMBB), massive Machine Type Communications (mMTC), and Ultra-Reliable and Low Latency Communications (URLLC). Each scenario has distinct service feature and requirement. High SE (up to 15bps/Hz for uplink and 30bps/Hz for downlink), massive connection (1 million devices/ km^2) and ultra reliability (10^{-5} packet error rate within 1ms user-plane latency) are key performance indicators (KPIs) for eMBB, mMTC and URLLC [5], respectively. The study on NOMA started from

the 3rd generation partnership project (3GPP) Release 14 (Rel-14) since September 2014, and it is ongoing at the study-item (SI) step of 3GPP Rel-15 until May 2018. The current target is to provide self evaluation against eMBB, mMTC and URLLC requirements and test environments for 5G new radio (NR) standardization. By the end of June 2019, 3GPP Rel-16 will accomplish the final 5G NR submission, including description template, compliance template, and self evaluation results.

The conventional orthogonal multiple access (OMA) technology allocates orthogonal time and frequency resources for multiple users, and each user's receiver can take advantage of this orthogonality to separate out its own signal from others simply. The NOMA technique utilizes the superposition coding principle to multiplex multiple users onto the same time and frequency resources. Therefore, NOMA can enlarge the number of connections by introducing controlled symbol collisions. Actually, NOMA can approach the capacity bound of the multi-user system more closely than OMA [6]. For the sake of intuition, consider a simple two-user uplink multiple access (MAC) system on the additive white gaussian noise

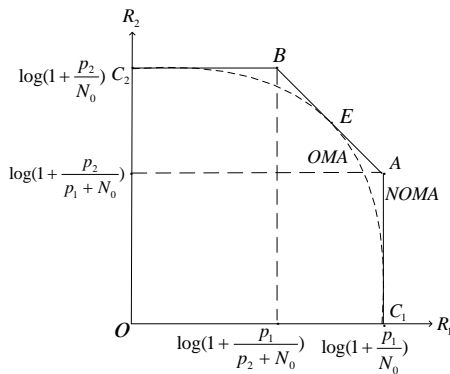


FIGURE 1: The capacity regions of OMA and NOMA.

(AWGN) channel. In Fig.1, the dashed curve and the real curve show the capacity regions for OMA and NOMA, respectively. p_i denotes the user's power, and N_0 denotes the single-sided power spectral density of the AWGN. The points C_1 and C_2 denote the maximum individual rate for user1 and user2, respectively, and the points A , B and E denote the maximum sum-rate. It is observed that the sum-rate of NOMA is usually higher than OMA except for one point E [7]. Hence the NOMA scheme based on superposition transmission has obvious advantages over OMA in terms of sum-rate, user-fairness and scheduling-flexibility.

Recently, many NOMA schemes were proposed for 5G, such as the power-domain NOMA [8], the low-density spreading (LDS) multiple access [9, 10], resource spread multiple access (RSMA) [11], low code rate and signature based shared access (LSSA) [12], multi-user shared access (MUSA) [13], non-orthogonal coded access (NOCA) [14], non-orthogonal coded multiple access (NCMA) [15], group orthogonal coded access (GOCA) [16], welch-bound spreading multiple access (WSMA) [17], pattern division multiple access (PDMA) [18], low density signature-signature vector extension (LDS-SVE) [19], sparse code multiple access (SCMA) [20], interleave-grid multiple access (IGMA) [21], interleave division multiple access (IDMA) [22], low code rate spreading (LCRS) [23], and repetition division multiple access (RDMA) [16]. These techniques all follow the superposition principle, and the difference among them is the user's signature design which is based on scrambling, spreading, coding, or interleaving distinctness. Therefore, we classify these schemes into four categories: scrambling-based, spreading-based, coding-based and interleaving-based NOMA[24].

The main contributions of this paper can be summarized as follows:

- We propose an overall classification of NOMA schemes which are key candidates in 5G according to their characteristics, systematically summarize the transceiver block diagram of each category, and detail basic principles, key features and transmission-reception algorithms of all NOMA schemes.

- We comprehensively compare all these NOMA and OMA schemes in terms of theoretical analysis, simulation performance and receiver complexity. Thus, some promising schemes and directions are suggested for the future 5G NOMA development.

The rest of this article is organized as follows. In Section II, we systematically summarize the key features of each category of the NOMA schemes, and discuss distinctness and similarity among them. In Section III, theoretical performance comparison is given based on the average mutual information (AMI) analysis. Section IV shows simulation results and the receiver complexity comparison of the NOMA schemes. Finally, conclusions are reached in Section V.

II. MULTIPLE ACCESS SYSTEM MODELS

In this section, key features of four NOMA categories are surveyed and compared comprehensively.

A. SCRAMBLING-BASED NOMA

Scrambling-based NOMA schemes consist of RSMA from Qualcomm, LSSA from ETRI and power-domain NOMA from NTT DoCoMo. The basic block diagram is shown in Fig.2. This scheme uses different scrambling signature for each user, and adopts a low-rate channel coding or repetition coding for multi-user decoding. The Scrambling operation is carried out after the modulation. Minimum mean square error with successive interference cancellation (MMSE-SIC) and elementary signal estimator (ESE) are used for the multi-user detection (MUD) [25]. The long scrambling sequences are used in RSMA. However, a long user signature causes high decoding complexity and latency. Thus the length of signature vectors is designed as short as possible in LSSA. Power-domain NOMA is considered as a special scrambling-based NOMA scheme whose scrambling-multiplication sequences are all "1".

RSMA utilizes the low cross-correlation properties of long pseudo-random scrambling codes. Actually, after the descrambling, the ratio of signal to interference power is directly proportional to the scrambling-code length. It is worth noting that each user can transmit signal at any time for the asynchronous RSMA. Depending on the application scenarios, it can adopt single-carrier RSMA or multi-carrier RSMA. Single-carrier RSMA can be used in the uplink access to reduce peak-to-average power ratio (PAPR) of UE. Multi-carrier RSMA is utilized in the downlink access to simplify the receiver complexity in the frequency-selective wireless fading channels. RSMA also can extend to multiple layers. Treating layers as virtual users, data is split into multiple parallel layers for each user. The complexity of multi-layer RSMA is higher than single-layer RSMA.

In the LSSA scheme, each user's information data is encoded by a low-rate channel coding, and then the output of channel encoder is multiplexed with the user specific signature which is either assigned to the user or chosen randomly in a pre-assigned signature pattern pool. All users' signatures have the same short vector length. This signature

pattern is unknown to other uplink users. By correlating with signature patterns, the base station is able to distinguish the overlapped user signals even if the transmission timing is different from each other. The LSSA also has a multi-carrier variant in order to exploit frequency diversity provided by wider bandwidth and achieve lower latency.

Power-domain NOMA can serve multiple users on the same radio resources by allocating different power to multiple users. The key idea of power-domain NOMA is to allocate more power to the far user with poorer channel condition due to the near-far effect. At the receiver side, those multiplexed users can be separated by the MMSE-SIC MUD method thanks to the large power-domain difference between near-far paired UEs.

B. SPREADING-BASED NOMA

MUSA from ZTE, NOCA from Nokia, NCMA from LGE, GOCA from Mediatek and WSMA from Ericsson all belong to the spreading-based NOMA schemes. Fig.3 shows its transceiver block diagram. The key feature is to use nonorthogonal short spreading sequences with relatively low cross-correlation for distinguishing multiple users, and the spreading sequences are non-sparse. The spreading sequences and the decoding algorithm are different for these schemes. The short spreading sequences of MUSA are taken in the complex-number domain. The spreading sequences used for NOCA are the low-correlation sequences defined in LTE [26]. The NCMA spreading sequences are obtained by Grassmannian line packing problem [27]. The WSMA spreading sequences are based on the Welch bound [28]. The GOCA spreading codes adopt grouped orthogonal se-

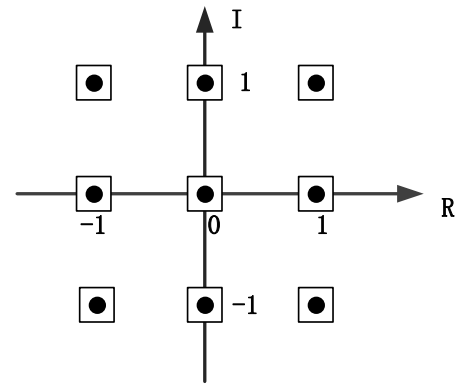


FIGURE 4: The elements of the complex spreading sequence.

quences.

In MUSA, modulation symbols of multiple users are spreaded by specially designed short sequences. All spreading symbols are transmitted over the same time-frequency resources. Multiple spreading sequences constitute a pool from which each user can randomly choose one. The spreading sequences of MUSA are complex-valued, in which the real part and imaginary part are both taken from a real-valued multi-level set with uniform distribution. For example, in Fig.4, for a 3-value set $\{-1, 0, 1\}$ in the real part and imaginary part, there are nine constellation points in the complex plane, and every complex element of the spreading sequence is randomly taken from these nine constellation points with independent equal probability to compose a pseudo-random

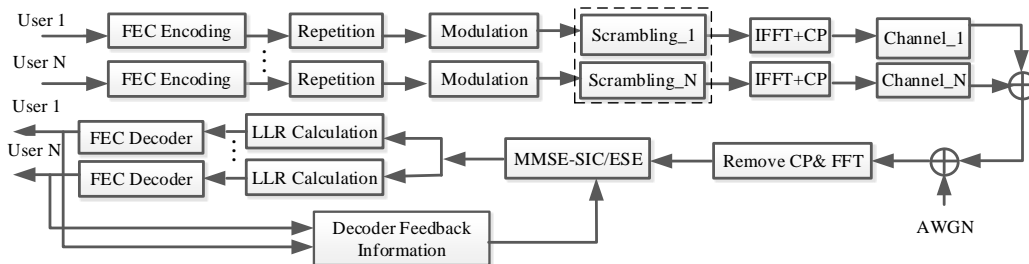


FIGURE 2: Scrambling-based NOMA transceiver block diagram.

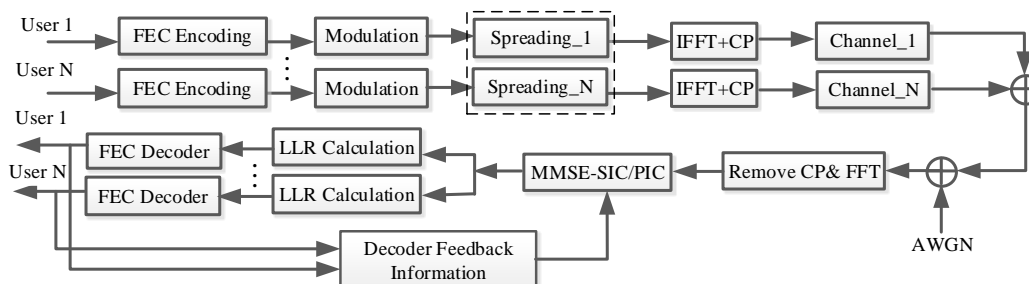


FIGURE 3: Spreading-based NOMA transceiver block diagram.

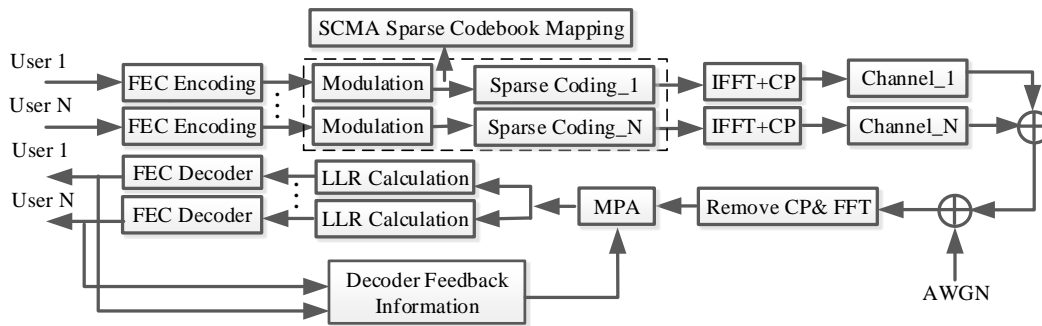


FIGURE 5: Coding-based NOMA transceiver block diagram.

short spreading sequence. At the receiver, the codeword-level SIC detection is used to separate out its own signal from overlapped signals.

The basic idea of NOCA is also that modulation symbols are spreaded using nonorthogonal sequences before transmission. The spreading sequences of NOCA are the reference signals defined in LTE, which are generated by cyclic shifts of a base sequence. The minimum spreading factor is 6. The original modulated data sequence is first converted into parallel subsequences. Afterwards, each subsequence is spreaded by nonorthogonal sequences and then mapped onto different subcarriers. The minimum mean square error with parallel interference cancellation (MMSE-PIC) receiver is used to decode each user's data from superimposed signals. NOCA provides plenty of spreading sequences, therefore can support higher overloading and facilitate to perform inter-cell coordination for interference mitigation.

NCMA's nonorthogonal spreading codes are obtained by Grassmannian line packing problem. The spreading codebook design aims to maximize the minimum chordal distance between spreading codes. The MMSE-PIC algorithm is used for NCMA at the receiver.

WSMA's spreading sequence design is based on the Welch bound to minimize the cross-correlation of the spreading sequences. At the receiver, the MMSE-SIC algorithm is utilized for MUD. Compare to the randomly spreading sequences in MUSA, WSMA spread sequences have relatively lower cross-correlation.

GOCA adopts a two-stage method to generate grouped orthogonal sequences, and then spreads modulated symbols into the same time and frequency resources. Orthogonal sequences and nonorthogonal sequences are used in the first and the second stage, respectively. GOCA's spreading sequences can be divided into different groups for multiple users, and each group has the same orthogonal sequence set and different nonorthogonal sequences. Thus, the users within each group remain orthogonality, while the users in different groups are nonorthogonal. GOCA also takes advantage of the MMSE-SIC algorithm for multi-user decoding.

C. CODING-BASED NOMA

Coding-based NOMA schemes are composed of PDMA from CATT, LDS-SVE from Fujitsu and SCMA from Huawei. The transceiver block diagram is depicted in Fig.5. Its distinct characteristic is to design the sparse codebook overlapped in the multiple (space, code, time or frequency) domains for the multiple users. The message passing algorithm (MPA) detector is implemented for MUD. The complexity order of MPA is exponential with the size of codebook and the degree of signal superposition on a given resource element (RE), which is very high for applications. A novel low-complexity iterative receiver based on expectation propagation algorithm (EPA) was proposed to reduce the complexity order from exponential to linear and can achieve nearly the same block error rate (BLER) performance [29].

PDMA, which is based on SAMA (SIC Amenable Multiple Access) technique [30], can be realized in multiple domains, including code domain, power domain, space domain or their combinations. It is a joint design of transmitter and receiver, especially with unequal diversity at the transmitter side and equal diversity at the receiver side. A PDMA pattern defines the mapping of transmitted data to a group of resources. As an example, a PDMA pattern matrix for 6 users on 4 REs is expressed as following

$$G = \begin{bmatrix} 1 & 1 & 1 & 0 & 0 & 0 \\ 1 & 1 & 0 & 1 & 0 & 0 \\ 1 & 1 & 1 & 0 & 1 & 0 \\ 1 & 0 & 0 & 1 & 0 & 1 \end{bmatrix}$$

Fig.6 shows the corresponding resource mapping process. The order of transmission diversity of the six users is 4, 3, 2, 2, 1, and 1, respectively. The pattern is designed to differentiate multiple users sharing the same resources. The performance depends on this pattern matrix of PDMA.

LDS-SVE is based on the original LDS to design a larger user signature vector. The extension can be accomplished by transforming and concatenating several element signature vectors into a larger signature vector. LDS-SVE maps user signature vectors across a few resource blocks (RBs) so as to exploit the time and frequency diversity from the channel variation.

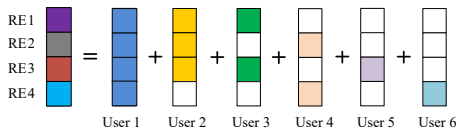


FIGURE 6: PDMA pattern for 6 users sharing on 4 REs.

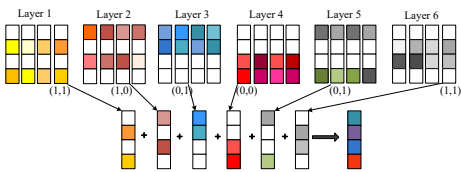


FIGURE 7: SCMA codebook bit-to-codeword mapping.

In SCMA, the coded bits of multiple data layer are directly mapped to the codewords according to the corresponding codebook set in the time and frequency domain. Fig.7 shows an example of a codebook set containing 6 codebooks for 6 data layers overlapped on 4 REs. Each codebook has 4 multi-dimensional complex codewords that correspond to 4 points of the Quadrature Phase Shift Keying (QPSK) constellation, respectively. The length of each codeword is 4, which is the same as the spreading length. The codeword of each layer is selected based on the input bit-sequence. It allows superposition of multiple symbols from different users on each RE. In Fig.7, there are 3 symbols from different UEs overlapped on each RE, and the order of transmission diversity is 2 for all six users. The corresponding mapping matrix F is shown as following

$$F = \begin{bmatrix} 0 & 1 & 1 & 0 & 1 & 0 \\ 1 & 0 & 1 & 0 & 0 & 1 \\ 0 & 1 & 0 & 1 & 0 & 1 \\ 1 & 0 & 0 & 1 & 1 & 0 \end{bmatrix}$$

The design of SCMA codebook is based on joint optimization of the sparse spreading codebook and the multi-dimensional rotational constellation to achieve additional “shaping” gain that is impossible for PDMA and LDS-SVE. Besides, in order to support multiple users with different business (such as coverage, connections and capacity), the irregular SCMA codebook is proposed, whose degree of layer’s RE is different. SCMA also uses the sparse spreading codebook to reduce the number of symbol collisions and thus lower the MUD complexity.

D. INTERLEAVING-BASED NOMA

IGMA from Samsung, RDMA from Mediatek, IDMA from Nokia and LCRS from Intel constitute the interleaving-based NOMA schemes, which originate from the basic concept IDMA [31, 32]. Their common distinct characteristic is to use different channel interleavers overlapped for multiple users and combine with a low-rate channel coding for multi-user decoding.

IDMA, as an original interleaving-based NOMA scheme, utilizes different random interleave patterns to separate users.

In the transmitter, the superposition of multiple symbols from all users is carried out on each RE, so the number of symbol collisions is equal to the number of users. In the receiver, the low-complexity ESE algorithm is implemented for MUD [25]. The low-complexity ESE provides log-likelihood ratio (LLR) estimates to the channel decoder, and in turn the channel decoder sends extrinsic LLR estimates to the ESE.

RDMA uses a simple cyclic-shift repetition pattern to separate different users’ signals and utilize both time and frequency diversity. It can be viewed as a special cyclic interleaving. The SIC receiver is utilized to decode each user’s data from superimposed signal.

In LCRS, the channel encoding, bit-level repetition, bit-level interleaving and modulation are carried out sequentially for each user. In the receiver, MMSE-PIC is performed for MUD.

The IGMA transceiver block diagram is shown in Fig.8. In the transmitter, the channel encoding, bit-level repetition, bit-level interleaving, modulation, zero padding and symbol-level interleaving are carried out sequentially for each user. In the receiver, the ESE algorithm is implemented for the multi-user decoding. Besides the interleaving pattern, IGMA also uses a sparse grid mapping pattern overlapped in the time and frequency domain, which is like LDS. Thus, IGMA is actually a mixture of interleaving-based and coding-based schemes. The sparse grid mapping pattern can reduce the symbol collisions and lower the detection complexity as compared with the conventional IDMA scheme.

III. THEORETICAL PERFORMANCE ANALYSIS

The AMI reflects the maximum information rate that can be reliably transmitted for given channel state information. In the single user case, the AMI between the signal after constellation mapping and that before the soft demapper is called coded modulation (CM)-AMI [33]. We extend this CM-AMI analysis to the multi-user case for evaluating the achievable sum-rate performance of the NOMA systems. $\mathbf{x} = [x_1, x_2, \dots, x_J]$ denotes the multi-user modulation symbol vector before the NOMA signature pattern, and $\mathbf{y} = (y_1, \dots, y_{K*N_r})$ represents the channel-output symbol vector at the receiver. J , K , M and N_r denote the number of users, the NOMA signature length, the order of modulation, and the number of receive antennas, respectively. Assuming equiprobable input of constellation points, $\Omega = \{\omega_0, \omega_1, \dots, \omega_{2^{MJ}-1}\}$ denotes the high-dimensional constellation set, then the CM-AMI can be computed as

$$\begin{aligned} I_{CM} &= \frac{1}{K} I(\mathbf{x}; \mathbf{y} | \mathbf{H}) \\ &= \frac{1}{K} (H(\mathbf{x}) - H(\mathbf{x} | \mathbf{y})) \\ &= \frac{J \log_2 M}{K} - \frac{1}{K} \mathbb{E}_{\mathbf{x}, \mathbf{y}, \mathbf{H}} \left\{ \log_2 \left[\frac{\sum_{w \in \Omega} P(\mathbf{y} | \mathbf{x} = w, \mathbf{H})}{P(\mathbf{y} | \mathbf{x}, \mathbf{H})} \right] \right\} \end{aligned} \quad (1)$$

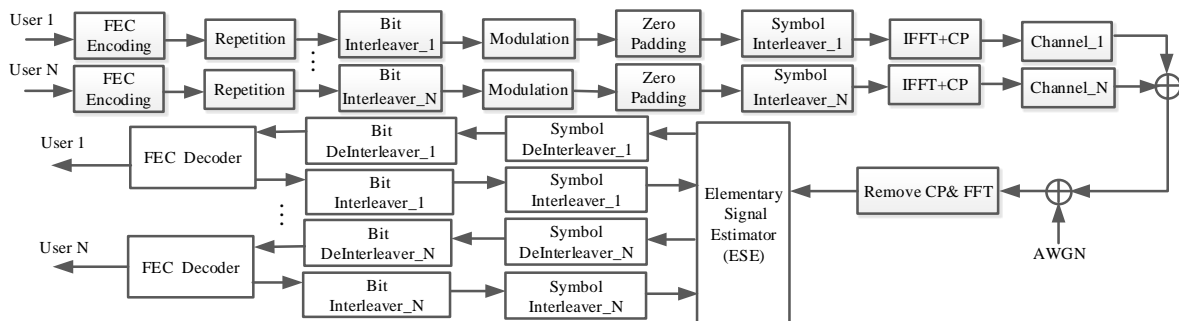


FIGURE 8: Interleaving-based IGMA transceiver block diagram.

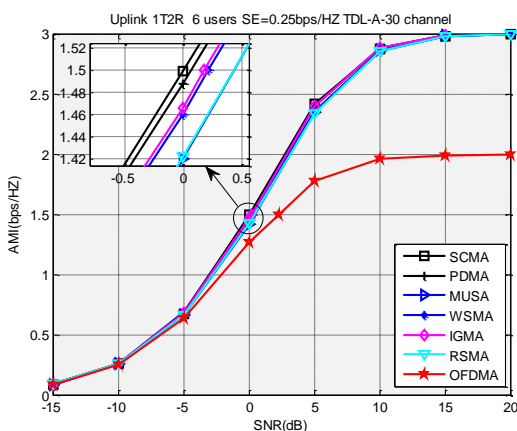


FIGURE 9: AMI comparison of NOMA and OFDMA under TDL-A-30 channel.

The Monte Carlo simulation technique is used to calculate the expectation in (1). Assuming a six-user uplink MAC system on the tapped delay line (TDL)-A-30 channel \mathbf{H} [34] and ideal channel estimation, the CM-AMI curves of the NOMA schemes and orthogonal frequency division multiple access (OFDMA) are shown in Fig.9. Some parameters without channel coding are shown in Table 1. Overloading factor is 150%, SE per user is 0.25bps/Hz, and the sum-rate is 1.5bps/Hz. The signal-to-noise ratio (SNR) is defined as the ratio of average total received multi-users' power to the noise power at each receive antenna for given bandwidth. The number of users, SE per user and transmission bandwidth are identical for both NOMA and OFDMA schemes to secure the comparison fairness. It can be observed that SCMA, PDMA, IGMA, WSMA, RSMA and MUSA can obtain 2.3dB, 2.25dB, 2.12dB, 2.09dB, 1.78dB, and 1.78dB SNR gains as compared with OFDMA at the achievable sum-rate 1.5bps/Hz, respectively. Thus, theoretically, the multi-user AMI analysis proves the significant superiority of NOMA schemes over OMA for given achievable sum-rate. In addition, the coding-based NOMA schemes have some performance advantage.

TABLE 1: Simulation parameters

Parameter	Value
Carrier frequency	2GHz
Length of information bits	216bits
System bandwidth	10MHz
Modulation	QPSK; 16QAM
Code rate	1/2; 3/4
Channel coding	LTE turbo code
Antenna configuration	1Tx; 2Rx
Channel model	TDL-A-30
Channel estimation	Ideal; Realistic
FFT length	1024
Overloading factor	150% ; 200%
Users	6; 8

IV. SIMULATION RESULTS AND COMPLEXITY COMPARISON

In this section, simulation results are provided to evaluate the error performance of the uplink NOMA schemes. The detailed simulation parameters are shown in Table 1. Multiple UEs are assumed to share the same 6 physical resource blocks (PRBs) to transmit signals. One PRB takes 12 OFDM symbols in time domain and 12 subcarrier in frequency domain.

A. RESULTS OF NOMA SCHEMES WITH IDEAL CHANNEL ESTIMATION

Assuming ideal channel estimation, Fig.10 and Fig.11 compare the BLER performance of NOMA and OFDMA schemes for 6 and 8 UEs, respectively. LTE turbo code is used [35]. In Fig.10, QPSK and half code rate for NOMA, QPSK and 3/4 code rate for OFDMA, overloading factor is 150%, SE per user is 0.25bps/Hz, and the sum-rate is 1.5bps/Hz. In Fig.11, QPSK and half rate for NOMA, 16QAM and half rate for OFDMA, overloading factor is 200%, SE per user is 0.25bps/Hz, and the sum-rate is 2.0bps/Hz. In Fig.10, SCMA, PDMA, IGMA, WSMA, RSMA and MUSA achieve 1.0dB, 1.0dB, 1.0dB, 1.0dB, 0.9dB, and 0.7dB SNR gain at target BLER 0.1 as compared with OFDMA, respectively, which coincides with the theoretical AMI analysis in Fig.9. In Fig.11, SCMA, PDMA, MUSA, RSMA and IGMA obtain 1.8dB, 1.8dB, 1.6dB, 1.55dB and 1.33dB SNR gain at target BLER 0.1 as compared with OFDMA, respectively. There-

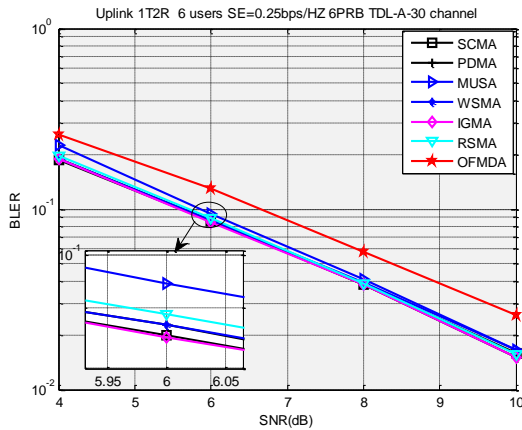


FIGURE 10: 6-user BLER performance comparison of NOMA under TDL-A-30 channel.

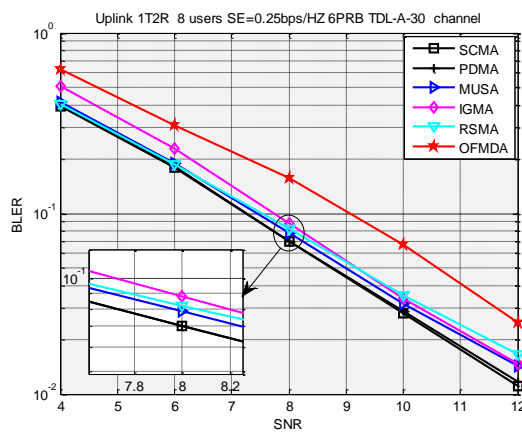


FIGURE 11: 8-user BLER performance comparison of NOMA under TDL-A-30 channel.

fore, the performance gains of NOMA schemes over OFDMA are significant. Besides, when the UE number increases, the OFDMA system needs to use higher order modulation so as to suffer serious performance loss, while NOMA with low order modulation can take full advantage of the superposition coding for higher overloading factor so as to have slight performance loss. Thus, comparing Fig.10 and Fig.11, the BLER performance difference between NOMA schemes and OFDMA grows with the increase of UE number.

B. RESULTS OF NOMA SCHEMES WITH REALISTIC CHANNEL ESTIMATION

For the sake of application, the performance results of turbo-coded NOMA schemes with realistic channel estimation are presented in Fig.13, and the 6-UE case is assumed as Fig.10. Fig.12 illustrates mapping process of reference signals for user j . The first OFDM symbol of a radio frame is used to transmit the LTE reference signal sequences [26], and the following 6 OFDM symbols are taken to send the signals of 6 UEs. The RE for reference signal of user j , which is

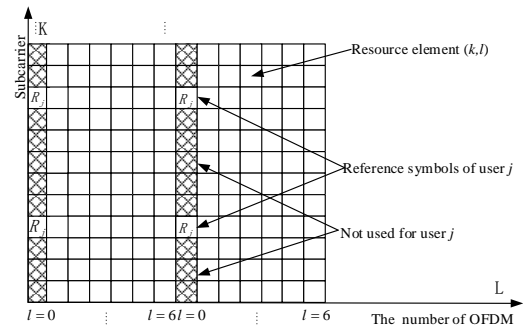


FIGURE 12: Mapping of reference signals for user j (normal cyclic prefix).

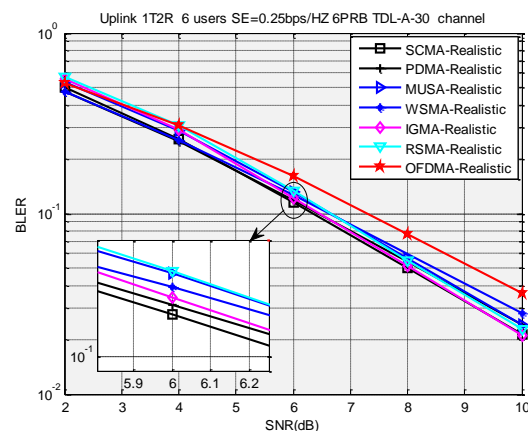


FIGURE 13: 6-user BLER performance comparison of NOMA under TDL-A-30 with realistic channel estimation.

denoted by R_j , separates from other UEs and distributes with 6-subcarrier spacing in the spectrum. Linear Minimum Mean Square Error (LMMSE) channel estimation and linear interpolation algorithm are used in the realistic channel estimation schemes. In Fig.13, SCMA, PDMA, IGMA, WSMA, RSMA and MUSA have 0.97dB, 0.85dB, 0.84dB, 0.68dB, 0.66dB and 0.65dB SNR gain as compared with OFDMA at target BLER 0.1, respectively. Therefore, NOMA schemes remain superior to OMA in terms of realistic channel estimation, which is very robust for the engineering application.

C. RESULTS OF GRANT-FREE NOMA SCHEMES

For the sake of robustness, the BLER performance results of grant-free turbo-coded NOMA schemes are depicted in Fig.14, and the 6-UE case is assumed as Fig.10. The allocation of codebook to each UE can be either fixed or random. For grant-based NOMA schemes, a base station (BS) allocates different codebooks to UEs, which is very complicated and requires the BS-scheduling to cause rather high latency. For grant-free NOMA schemes, UEs randomly choose the codebook without the BS-scheduling, which is much simpler and very suitable for low-latency applications. Actually, MUSA, IGMA and RSMA are grant-free by nature.

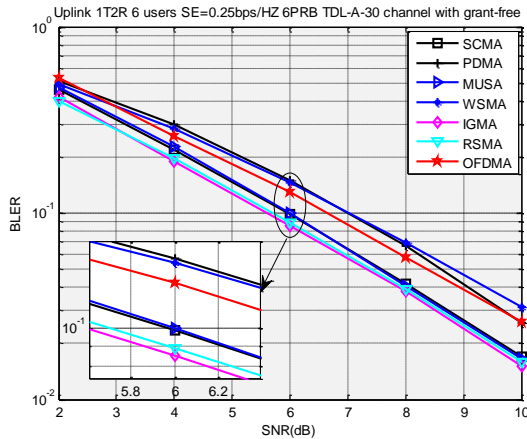


FIGURE 14: 6-user BLER grant-free performance comparison of NOMA under TDL-A-30 channel .

But some codebook, pattern and spreading collisions will occur for grant-free SCMA, PDMA and WSMA, respectively, which will cause some performance loss. Taking grant-based OFDMA as a baseline, IGMA, SCMA, MUSA and RSMA remain 1.0dB, 0.9dB, 0.6dB, and 0.4dB SNR gain at target BLER 0.1, respectively, while PDMA and WSMA suffer 0.3dB and 0.4dB SNR loss, respectively. Hence, IGMA, SCMA, MUSA and RSMA are robust for the grant-free scenario.

D. RESULTS OF LDPC-CODED NOMA SCHEMES

Powerful low density parity check (LDPC) codes are adopted in the latest 5G standard [36]. The BLER performance of the LDPC-coded NOMA schemes is evaluated in Fig.15, and the 6-UE case is assumed as Fig.10. Assuming ideal channel estimation and grant-based scheme, LDPC-coded SCMA, PDMA, WSMA, IGMA, MUSA and RSMA obtain 0.9dB, 0.9dB, 0.9dB, 0.9dB, 0.9dB and 0.8dB at target BLER 0.1 under TDL-A-30 channel as compared with LDPC-coded OFDMA, respectively. Actually, the LDPC-coded NOMA schemes have almost the same BLER and SNR gain as the corresponding turbo-coded NOMA schemes in Fig.10. Thus, NOMA schemes are robust for 5G LDPC codes.

E. COMPLEXITY COMPARISON

The receiver decoding algorithms of NOMA schemes are summarized in Table 2. Coding-based NOMA schemes, such as SCMA, PDMA and LDS-SVE, employ the MPA receiver for the iterative detection combining with the channel decoding, and the number of external iteration and that of internal iteration are 4 and 3, respectively. RSMA, IDMA and IGMA use the ESE algorithm for the iterative detection, and the number of external iteration is 4. LCRS, NOCA and NCMA utilize the MMSE-PIC algorithm without external iteration. For MUSA and WSMA, the MMSE-SIC without external iteration is used. For the 6-UE case in Fig.10, we compute the total NOMA detection and turbo decoding complexity

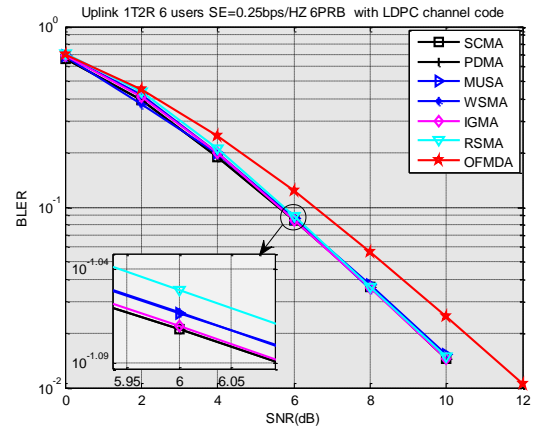


FIGURE 15: 6-user LDPC-coded BLER performance comparison of NOMA under TDL-A-30 channel .

of NOMA schemes at the receiver, including multiplication, addition and comparison operations [37]. For the sake of statistic, one comparison operation is equal to one addition operation, while one multiplication operation equals eight addition operations. Taking the external and internal iterations into account, Table 2 shows the decoding operations per information bit and the relative complexity percentage as compared to SCMA. Obviously, the complexity of SCMA is highest, while MUSA and WSMA have almost the same lowest complexity. However, the overall receiver detection/decoding operations are on the same complexity order for all NOMA schemes.

V. CONCLUSION

In this article, the latest NOMA schemes proposed for the 5G standard are comprehensively studied and compared. Firstly, we classify these schemes into four categories: scrambling-based, spreading-based, coding-based and interleaving-based NOMA schemes. Key characteristics and transceiver algorithms of each NOMA scheme are detailed and compared. Theoretically, it is proved by the multi-user AMI analysis that NOMA schemes can obtain significant SNR gain for given achievable sum-rate. Practically, comprehensive simulation results verify such remarkable gain, even for the realistic channel estimation and the grant-free scenario. Complexity comparison of NOMA schemes is also given. It seems that coding-based and spreading-based NOMA schemes have some advantages in terms of bigger connectivity and robustness. However, we think that there is still some improvement room for these schemes to combine the NOMA signatures (patterns) with 5G-adopted powerful LDPC codes, high-order modulation, and incremental redundancy hybrid ARQ (HARQ) schemes.

REFERENCES

- [1] G. Eason, Boccardi, R. W. Heath Jr, A. Lozano, T. L. Marzetta, and P. Popovski, "Five disruptive technology

TABLE 2: Complexity comparison

NOMA	Receiver algorithm	Multiplication per bit	Addition per bit	Comparison per bit	Operations per bit	Percentage
SCMA	MPA	300	3634	956	6990	100%
RSMA	ESE	364	2264	228	5404	77.3%
PDMA	MPA	235	2364	952	5196	74.3%
IGMA	ESE	278	2224	228	4676	66.9%
WSMA	MMSE-SIC	387	921	229	4246	60.7%
MUSA	MMSE-SIC	387	921	229	4246	60.7%

- directions for 5G,” *IEEE Commun. Mag.*, vol. 52, no. 2, pp. 74–80, Feb. 2014.
- [2] W. Shin, M. Vaezi, B. Lee, D. J. Love, J. Lee and H. V. Poor, “Non-Orthogonal Multiple Access in Multi-Cell Networks: Theory, Performance, and Practical Challenges,” *IEEE Commun. Mag.*, vol. 55, no. 10, pp. 176–183, Oct. 2017.
- [3] Zhiguo Ding, Yuanwei Liu, Jinho Choi, Qi Sun, Maged El-kashlan, Chih-Lin I, and H. Vincent Poor, “Application of Non-Orthogonal Multiple Access in LTE and 5G Networks,” *IEEE Commun. Mag.*, vol. 55, no. 2, pp. 185–191, February 2017.
- [4] Z. Ding, X. Lei, G. K. Karagiannidis, R. Schober, J. Yuan and V. K. Bhargava, “A Survey on Non-Orthogonal Multiple Access for 5G Networks: Research Challenges and Future Trends,” *IEEE Journal on Selected Areas in Communications*, vol. 35, no. 10, pp. 2181–2195, Oct. 2017.
- [5] 3rd Generation Partnership Project; Technical Specification Group Radio Access Network; Study on Scenarios and Requirements for Next Generation Access Technologies (Release 14), document 3GPP TR 38.913 V14.3.0, Jun.2017.
- [6] D. Tse and P. Viswanath, *Fundamentals of Wireless Communication*. Cambridge, UK: Cambridge Univ. Press, 2005, pp. 228–240.
- [7] L. Dai, B. Wang, Y. Yuan, S. Han, C. I. I and Z. Wang, “Non-orthogonal multiple access for 5G: solutions, challenges, opportunities, and future research trends,” *IEEE Commun. Mag.*, vol. 53, no. 9, pp. 74–81, Sep. 2015.
- [8] Initial views and evaluation results on non-orthogonal multiple access for NR, document R1-165175, NTT DOCOMO, 3GPP, May 2016.
- [9] R. Hoshyar, F.P. Wathan, and R. Tafazolli, “Novel low-density signature for synchronous CDMA systems over AWGN channel,” *IEEE Trans.Signal Process.*, vol. 56, no. 4, pp. 1616–1626, Apr. 2008.
- [10] J. Van De Beek and B. M. Popovic, “Multiple access with low-density signatures,” in *Proc. IEEE GLOBECOM*, Dec. 2009, pp. 1–6.
- [11] Resource spread multiple access, document R1-164688, Qualcomm, 3GPP, May 2016.
- [12] Low code rate and signature based multiple access scheme for New Radio, document R1-164869, ETRI, 3GPP, May 2016.
- [13] Contention-based non-orthogonal multiple access for UL mMTC, document R1-164269, ZTE, 3GPP, May 2016.
- [14] Non-orthogonal multiple access for New Radio, document R-165019, Nokia, 3GPP, May 2016.
- [15] Considerations on DL/UL multiple access for NR, document R1-162517, LGE, 3GPP, Apr. 2016.
- [16] New uplink non-orthogonal multiple access schemes for NR, document R1-167535, Mediatek, 3GPP, Aug. 2016.
- [17] NOMA Design principles and performance, Ericsson, IMT-2020, Beijing, China, 14 Jun. 2017.
- [18] Candidate Solution for New Multiple Access, document R1-163383, CATT, 3GPP, Apr. 2016.
- [19] Initial LLS results for UL non-orthogonal multiple access, document R1-164329, Fujitsu, 3GPP, May 2016.
- [20] LLS results for uplink multiple access, document R1-164037, Huawei, 3GPP, May 2016.
- [21] Non-orthogonal multiple access candidate for NR, document R1-163992, Samsung, 3GPP, May 2016.
- [22] Performance of Interleave Division Multiple Access (IDMA) in combination with OFDM family waveforms, document R1-165021, Nokia, 3GPP, May 2016
- [23] Multiple access schemes for new radio interface, document R1-162385, Intel, 3GPP, Apr. 2016.
- [24] Classification of candidate UL non-orthogonal MA schemes, document R1-167445, China Telecom, 3GPP, Aug. 2016.
- [25] Li Ping, Lihai Liu, K. Y. Wu, and W. K. Leung, “On Interleave-division Multiple-Access,” in *Proc. IEEE International Conference on Communications (ICC)*, Jun. 2004, pp. 2869–2873.
- [26] 3rd Generation Partnership Project; Technical Specification Group Radio Access Network; Evolved Universal Terrestrial Radio Access (E-UTRA); Physical Channels and Modulation (Release 13), document 3GPP TS36.211.version 13.1.0, Mar. 2016.
- [27] Ahmed Medra and Timothy N. Davidson, “Flexible Codebook Design for Limited Feedback Systems via Sequential Smooth Optimization on the Grassmannian Manifold,” *IEEE Transactions on Signal Processing*, vol. 62, no. 5, pp. 1305–1318, Mar. 2014.
- [28] L. Welch, “Lower bounds on the maximum cross correlation of signals,” *IEEE Transactions on Information Theory*, vol. 20, no. 3, pp. 397–399, May 1974.
- [29] X. Meng, Y. Wu, Y. Chen and M. Cheng, “Low Com-

- plexity Receiver for Uplink SCMA System via Expectation Propagation,” in Proc. IEEE Wireless Communications and Networking Conference (WCNC), Mar. 2017, pp. 1–5.
- [30] Xiaoming Dai, Shanzhi Chen, Shaohui Sun, Shaoli Kang, Yinmin Wang, Zukang Shen, and Jin Xu, “Successive Interference Cancellation Amenable Multiple Access (SAMA) for Future Wireless Communications,” in Proc. IEEE International Conference on Communication Systems (ICCS), Nov. 2014, pp. 222–226.
- [31] Li Ping, Lihai Liu, Keying Wu and W. K. Leung, “Interleave division multiple-access,” IEEE Transactions on Wireless Communications, vol. 5, no. 4, pp. 938–947, Apr. 2006.
- [32] Li Ping, “Interleave-division multiple access and chip-by-chip iterative multi-user detection,” IEEE Commun. Mag., vol. 43, no. 6, pp. S19–S23, Jun. 2005.
- [33] Qiuliang Xie, Jian Song, Kewu Peng, Fang Yang, and Zhaocheng Wang, “Coded modulation with signal space diversity,” IEEE Transactions on Wireless Communications, vol.10, no.2, pp.660–669, Feb. 2011.
- [34] 3rd Generation Partnership Project; Technical Specification Group Radio Access Network; Study on channel model for frequency spectrum above 6 GHz (Release 14), document 3GPP TR38.900.version 14.2.0, Dec. 2016.
- [35] 3rd Generation Partnership Project; Technical Specification Group Radio Access Network; Evolved Universal Terrestrial Radio Access (E-UTRA); Multiplexing and channel coding (Release 14), document 3GPP TS 36.212 V14.5.0, Dec. 2017.
- [36] 3rd Generation Partnership Project; Technical Specification Group Radio Access Network; NR; Multiplexing and channel coding (Release 15), document 3GPP TS38.212.version 1.2.1, Dec. 2017.
- [37] P. Robertson, E. Villebrun, and P. Hoeher, “A comparison of optimal and sub-optimal MAP decoding algorithms operating in the log domain” in Proc. IEEE International Conference on Communications (ICC), Jun. 1995, pp. 1009–1013.

...